

Original Research

Investigating Endocrine Disrupting Impacts of Nine Disinfection Byproducts on Human and Zebrafish Estrogen Receptor Alpha

Sang-Ah Lee^{1,2,†}, Chang Gyun Park^{1,†}, Maranda Esterhuizen^{1,3,4}, Ian Choi¹,
Chang Seon Ryu¹, Ji Hun Yang⁵, Young Jun Kim^{1,*}¹Korea Institute of Science and Technology Europe (KIST Europe) Forschungsgesellschaft GmbH, Joint Laboratory of Applied Ecotoxicology, Environmental Safety Group, Universität des Saarlandes, 66123 Saarbrücken, Germany²Office of Islands and Coastal Biology Research, Honam National Institute of Biological Resources (HNIBR), 58762 Mokpo, Republic of Korea³Ecosystems and Environment Research Programme, Faculty of Biological and Environmental Sciences, University of Helsinki, 15140 Lahti, Finland⁴Clayton H. Riddell Faculty of Environment, Earth, and Resources, University of Manitoba, Winnipeg, MB R3T 2N2, Canada⁵Next&Bio Inc., 02841 Seoul, Republic of Korea*Correspondence: youngjunkim@kist-europe.de (Young Jun Kim)

†These authors contributed equally.

Academic Editor: Filomena Mottola

Submitted: 26 December 2022 Revised: 25 February 2023 Accepted: 1 March 2023 Published: 13 March 2023

Abstract

Background: Disinfection byproducts (DBPs) cause endocrine disruption via estrogenic or anti-estrogenic effects on estrogen receptors. However, most studies have focused on human systems, with little experimental data being presented on aquatic biota. This study aimed to compare the effects of nine DBPs on zebrafish and human estrogen receptor alpha (zER α and hER α). **Methods:** *In vitro* enzyme response-based tests, including cytotoxicity and reporter gene assays, were performed. Additionally, statistical analysis and molecular docking studies were employed to compare ER α responses. **Results:** Iodoacetic acid (IAA), chloroacetonitrile (CAN), and bromoacetonitrile (BAN) showed robust estrogenic activity on hER α (maximal induction ratios of 108.7%, 50.3%, and 54.7%, respectively), while IAA strongly inhibited the estrogenic activity induced by 17 β -estradiol (E2) in zER α (59.8% induction at the maximum concentration). Chloroacetamide (CAM) and bromoacetamide (BAM) also showed robust anti-estrogen effects in zER α (48.1% and 50.8% induction at the maximum concentration, respectively). These dissimilar endocrine disruption patterns were thoroughly assessed using Pearson correlation and distance-based analyses. Clear differences between the estrogenic responses of the two ER α s were observed, whereas no pattern of anti-estrogenic activities could be established. Some DBPs strongly induced estrogenic endocrine disruption as agonists of hER α , while others inhibited estrogenic activity as antagonists of zER α . Principal coordinate analysis (PCoA) showed similar correlation coefficients for estrogenic and anti-estrogenic responses. Reproducible results were obtained from computational analysis and the reporter gene assay. **Conclusions:** Overall, the effects of DBPs on both human and zebrafish highlight the importance of controlling their differences in responsiveness for estrogenic activities including the water quality monitoring and endocrine disruption, as DBPs have species-specific ligand-receptor interactions.

Keywords: disinfection byproduct; iodoacetic acid (IAA); chloroacetonitrile (CAN); bromoacetonitrile (BAN); estrogenic effects

1. Introduction

Wastewater generation is an unavoidable consequence of anthropogenic activities; however, concerns about the impact on human health of harmful microbes in wastewater are growing [1]. One of the purposes of wastewater management is to remove harmful microbes (bacteria and viruses) from the wastewater; therefore, chemical disinfectants are inevitably used in wastewater management for disinfection [2]. Wastewater treatment plants (WWTPs) commonly employ chemical disinfection processes due to their effectiveness [3]. Chlorination and chloramination are chemical disinfection processes with a long history of application. These chemicals undergo reactions, generating halogenated disinfection byproducts (DBPs) including trihalomethanes (THMs), haloacetic acids (HAAs), haloacetamides (HAMS), and haloacetonitriles (HANs). Thus,

DBPs have been detected widely in drinking water, swimming pools, water treatment plants, source water, and landfill leachate [4–8]. The previous studies reported that DBPs were detected with various ranges of concentrations (a few micrograms per liter to hundreds of micrograms per liter). Unfortunately, DBPs can cause adverse effects on living organisms, and some regulations have been introduced to reduce the use of disinfectants due to the significant hazards related to various DBPs [9].

To reduce the generation of DBPs, alternative disinfection processes have been employed, such as ultraviolet (UV) irradiation and ozonation. UV irradiation meets the required standards for low generation of DBPs, and ozonation has a lower risk than chlorination and chloramination in terms of DBP formation from natural organic matter (NOM) [10]. However, barriers to the implementation of such alternative treatments have been identified, including



imperfect disinfection results for specific microbes. Eischeid *et al.* [11] demonstrated that UV-resistant viruses, such as adenoviruses with double-stranded DNA, can infect host cells even after DNA damage caused by UV irradiation. Ozonation generates free radicals and ions, including HO·, HO₂·, O⁻, and O₂, which are necessary for disinfection [12]. The ozone reaction is generally rapid, and the concentration of ozone is halved within the first 30 s [13]. Removal of fungi is also challenging due to resistance against ozonation. Thus, UV irradiation and ozonation have significant limitations for the disinfection of harmful microbes. Chemical-based disinfectants used since the early 1900s are still widely employed in WWTPs after biological processes to reduce levels of harmful microbes that may induce waterborne diseases [14].

Among DBPs, THMs have received considerable attention in recent years due to their associated health risks [15]. Numerous toxicological and epidemiological studies have been conducted on THMs in drinking water [15]. Furthermore, control of THM discharge in final effluent from WWTPs has become a critical issue in the United States [16]. Among other halogenated DBPs, HAAs, HAMs, and HANs are partially regulated or unregulated by the United States Environmental Protection Agency [17,18]. The toxicity of DBPs has been investigated *in vitro* and *in vivo*, indicating that DBPs cause cytotoxicity, genotoxicity, mutagenicity, and developmental toxicity [19–21]. Particularly, our previous research evaluated the endocrine disruption potency of DBPs, including HAAs, HAMs, and HANs. We found that some DBPs showed agonistic or antagonistic effects on human estrogen receptor α (hER α) [22,23]. Estrogen-derived functions, which are associated with the ERs, play critical roles in homeostasis, growth, reproduction, and the regulation of the female reproductive system [24–27]. Owing to these properties, exogenous chemicals mimic estrogenic hormones and interrupt the endocrine system. Thus, the chemicals result in adverse effects on humans and other organisms [28]. The risks posed by endocrine-disrupting chemicals (EDCs) are continuously increasing [29]. Moreover, numerous studies reported that EDCs associated with ERs disrupt hormone systems and cause population changes in aquatic organisms [30,31]. Considering our previous studies, DBPs can adversely affect the endocrine system in not only humans, but also in aquatic organisms. Particularly, DBPs can significantly have a great influence on fish species, because fishes are susceptible to exposure and accumulation of chemicals in the aquatic environment. Such freshwater species can be directly impacted due to major wastewater effluent with DBPs [32]. However, there is still a lack of evidence on their endocrine disruptive activities, especially reproductive toxicity in aquatic organisms. In this study, we aim to investigate the binding effects of nine DBPs on the zebrafish and human ERs, resulting in different interactions across species by using ER α reporter gene assay in terms

of estrogenic and anti-estrogenic activities. This study will shed light on the species-specific activity of DBP-induced endocrine disruption.

2. Materials and Methods

2.1 Chemical Preparation

Cell viability and endocrine-disrupting effects are closely linked to chemical purity. Iodoacetic acid (IAA), iodoacetamide (IAM), iodoacetonitrile (IAN), chloroacetic acid (CAA), chloroacetamide (CAM), chloroacetonitrile (CAN), bromoacetic acid (BAA), bromoacetamide (BAM), and bromoacetonitrile (BAN) (>97% purity; Sigma-Aldrich, St. Louis, MO, USA) were dissolved in dimethyl sulfoxide (>99.9% purity, D8418; Sigma-Aldrich). Given its influence on the results, chemical purity was ensured through experimental evaluation of impacts on both cell viability and endocrine-disrupting effects (**Supplementary Fig. 1**).

2.2 Human Embryonic Kidney 293 (HEK293) Cell Culture

The HEK293 cell line was provided by the American Type Culture Collection (CRL-1573; ATCC, Manassas, VA, USA). The cell line was used for transfection as a host for the zER α construct. The HEK293 cell line (ATCC#CRL-1573) used for transfection as a host for the zER α construct was obtained from the American Type Culture Collection (ATCC, Manassas, VA, USA). HEK293 cells were cultured in Dulbecco's modified Eagle's medium (DMEM; ThermoFisher Scientific, Waltham, MA, USA) with 10% fetal bovine serum (FBS, A4136401; ThermoFisher Scientific) and 1% penicillin–streptomycin (15140122; ThermoFisher Scientific, Waltham, MA, USA) at 37 °C and 5% CO₂. Mycoplasma testing has been done for the cell line using MycoAlert™ PLUS Mycoplasma Detection Kit (LT07; Lonza, Walkersville, MD, USA). The used cell line has been authenticated by using Short Tandem Repeat (STR) analysis.

2.3 Cell Viability

Cell viability was determined prior to evaluating estrogenic and anti-estrogenic activities of DBPs. Each prepared stock of DBPs was diluted at a ratio of 10⁻² in DMEM (the range of working concentrations was 0.5–500 μ M). Cells were seeded in a 96-well plate at 1 \times 10⁴ cells/well and incubated under conditions of 37 °C and 5% CO₂. After overnight incubation, working concentrations of DBPs that did not exceed 0.5% (v/v) were applied to the cells for 24 h. Cell viability was assessed using Cell Counting Kit-8 (Dojindo, Kumamoto, Japan) according to the manufacturer's manual and measured at 450 nm using a microplate reader (SPARK; TECAN, Männedorf, Switzerland).

2.4 Transfection Methodology

First, HEK293 cells were transfected with the pGreen-Fire Lenti-reporter plasmid (pGF2-ERE-rFLuc-T2A-GFP-mPGK-Puro; TR455VA-P; System Biosciences, Palo Alto, CA, USA). The plasmid was designed to express red-shifted luciferase and the green fluorescent protein (GFP) reporter under the control of estrogen response element (ERE), and to have resistance to puromycin. Briefly, cells were seeded at a density of 3×10^5 cells/well in a 6-well plate (145380; ThermoFisher Scientific, Waltham, MA, USA) prior to transfection. After overnight incubation, the medium containing the virus was removed and treated with 5 $\mu\text{g}/\text{mL}$ polybrene (TR-1003; Sigma-Aldrich, St. Louis, MO, USA) for 8 h. The virus-containing medium was aspirated and the transfected cells were incubated overnight for recovery prior to treatment with 5 $\mu\text{g}/\text{mL}$ puromycin (J67236; ThermoFisher Scientific, Waltham, MA, USA). Next, HEK293-ERE cells were transfected with the piggyBac transposon gene expression system. This plasmid (VB160216-10057; VectorBuilder Inc., Chicago, IL, USA) encodes a hyperactive version of the piggyBac transposase. The zER α expression vector was custom-cloned by VectorBuilder (pPB-Neo-CAG>zER α , VB210426-1022cns). Cells were seeded at 1×10^5 cells/well in a 6-well plate. After overnight incubation, 0.75 μL of Lipofectamine 3000 reagent (L3000; ThermoFisher Scientific, Waltham, MA, USA) and 1 μg of the vector were mixed in 250 μL of OptiMEM medium (31985070; GIBCO, Grand Island, NY, USA) and incubated for 15 min to form a DNA-lipid complex. The complex was added to each well and incubated for 6 h. The complex medium was discarded, and cells were cultured with their regular medium for recovery overnight prior to treatment with 10 $\mu\text{g}/\text{mL}$ puromycin and 2 $\mu\text{g}/\text{mL}$ neomycin (N1142; Sigma-Aldrich, St. Louis, MO, USA), respectively. Finally, the transfected cells (HEK293-ERE-zER α) were collected for testing.

2.5 Luciferase Reporter Assay for Agonistic and Antagonistic Activities

HEK293-ERE-zER α cells were used to evaluate the (anti) estrogenic activities of DBPs. E2 (3301; Sigma-Aldrich, St. Louis, MO, USA) and 4-hydroxytamoxifen (HT, T176; Sigma-Aldrich, St. Louis, MO, USA) were selected as reference chemicals with agonistic and antagonistic activities, respectively. Cells were exposed to half-logarithmic (3.16-fold) dilutions of the reference chemicals and DBPs. The exposure ranges were 10^{-13} to 10^{-9} M for E2, 10^{-9} to 10^{-6} M for HT, and 10^{-11} to 10^{-6} M for DBPs. To investigate antagonistic activity, E2 was added to the culture medium at a fixed concentration (10^{-10} M). The test chemicals were dissolved in dimethylsulfoxide (DMSO) at working concentrations that did not exceed 0.5% (v/v). Cells were seeded at a concentration of 1×10^4 cells/well in a 96-well plate and incubated under conditions of 37 °C and 5% CO₂. After overnight incubation,

the working concentrations were added at a 1:1 ratio to the medium in each well and cultured for 24 h. Cells were lysed with passive lysis buffer (E194A; Promega, Madison, WI, USA) after washing with phosphate-buffered saline and the lysates were used to evaluate luciferase activity with the Luciferase Reporter Assay System (E151A; Promega, Madison, WI, USA). Luminescence was measured as relative luminescence using a microplate reader (SPARK; TECAN, Männedorf, Switzerland) with an integration time of 3 seconds and settling time of 1 second.

2.6 Principal Coordinate Analysis

Principal coordinate analysis (PCoA) was conducted based on the Bray–Curtis dissimilarity. The open source R package *vegan* 2.5-7 was used for distance calculations (<https://cran.r-project.org/web/packages/vegan/vegan.pdf>).

2.7 Homology Modeling and Molecular Docking

The crystal structure of hER α (Protein Data Bank [PDB] ID: 2YJA) was selected as the template for molecular docking and homology modeling. The crystal structure was the hER α ligand-binding domain (LBD) with E2 as the ligand [33]. The LBD structure of zER α was structuralized through homology modeling [34]. First, the LBD sequence of the target protein zER α (P57717) was validated against the UniProt database to generate the homology model. The query sequence was inserted into the Protein Basic Local Alignment Search Tool (BLASTp) to obtain an optimal template. hER α -LBD (2YJA) was chosen as the optimal template based on the BLASTp search. MODELLER 9.25, which can conduct comparative protein structure modeling if certain spatial restraints are satisfied, was used to create a homology model for zER α -LBD. This modeling tool forecasts the 3D structure of an input protein target sequence based primarily on its alignment with one or more proteins with known template structures to generate a zER α -LBD model [35]. The LBD sequence of zER α and its template structure (2YJA) were used as the inputs to MODELLER v9.25 (<https://salilab.org/modeller/9.25/release.html>). When alignment was completed, the program automatically calculated a 3D model of the target using its automodel function [35]. MODELLER generates 3D models accommodating all main chain and side chain non-hydrogen atoms based on the input target sequence. Ten candidate models were created, and the structure with the lowest Discrete Optimized Protein Energy score was selected as the zER α -LBD model for molecular docking [36]. The quality of the generated homology model was assessed using the computational protocols ERRAT [37], PROCHECK [38], and ProSA [39]. The hER α -LBD and zER α -LBD structures thus generated were used for molecular docking. Receptor preparation was conducted by discarding the crystallographic water molecules and ligand. Missing hydrogen atoms and charges were added during receptor preparation. E2 and DBPs were selected as the

test ligands, and their structures were downloaded from the PubChem database (E2: 5757, IAA: 5240, IAM: 3727, IAN: 69356, CAA: 6580, CAM: 6580, CAN: 7856, BAA: 6227, BAM: 69632, and BAN: 11534). Each structure was obtained in structure data file format and their geometries were improved using the MM2 energy minimization method. The files were changed to PDB format using Discovery Studio Visualizer 2016 (Accelrys Software Inc., San Diego, CA, USA). Molecular docking was performed using AutoDock Vina (The Scripps Research Institute, San Diego, CA, USA), which assumes that a receptor is rigid and ligands are flexible during molecular docking. This method employs a docking configuration file that includes protein and ligand information along with grid box properties [40]. Root-mean-square deviation (RMSD) values <1.0 Å indicated favorable binding free energies. The grid size was set to 40 points in each of the x, y, and z directions, with a grid spacing of 1.0 Å. The energy map was constructed using the distance-dependent function of the dielectric constant, and the default settings were used for all other parameters. All docked positions were computed using rankings based on binding energies. The position with the lowest binding energy was selected and aligned with the receptor structure for further analysis.

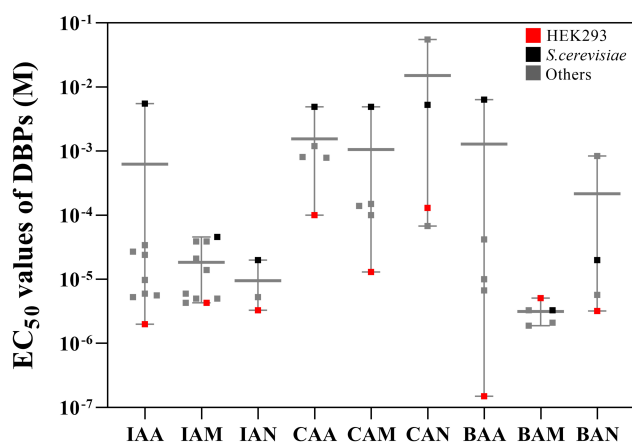


Fig. 1. Comparison of the median lethal dose among organisms. Red squares represent HEK293; black squares represent *S. cerevisiae*, and gray squares indicate other organisms from previous studies. Abbreviations: IAA, iodoacetic acid; IAM, iodoacetamide; IAN, iodoacetoneitrile; CAA, chloroacetic acid; CAM, chloroacetamide; CAN, chloroacetoneitrile; BAA, bromoacetic acid; BAM, bromoacetamide; BAN, bromoacetoneitrile.

3. Results

3.1 Comparison of Cytotoxicity among DBPs

The cytotoxicity of DPBs was evaluated on HEK293 cells to determine the ranges of exposure concentrations for testing endocrine disruption. The cell viability of exposed cells was presented with concentration-response curves in

Supplementary Fig. 2. The half-maximum effective concentration (EC_{50}) values for DBPs were as follows: 5.32×10^{-6} M for IAA, 4.35×10^{-6} M for IAM, 5.26×10^{-6} M for IAN, 1.03×10^{-4} M for CAA, 1.30×10^{-5} M for CAM, 1.29×10^{-4} M for CAN, 1.55×10^{-5} M for BAA, 5.13×10^{-6} M for BAM, and 5.72×10^{-6} M for BAN, respectively. The result of EC_{50} values indicated differences in cytotoxicity between DBPs. The DBPs containing iodine and bromine showed higher cytotoxicity than chlorine-containing DBPs. Iodine- and bromine-containing DBPs exhibited similar cytotoxicity except for BAA. We also investigated the cytotoxicity of DBPs evaluated from other model systems and compared the EC_{50} values (Table 1 (Ref. [20,22,23,41–53]), and Fig. 1). Although some EC_{50} values exhibited variance between model systems, the data showed a similar tendency to the present result. Thus, we confirmed that the iodine- and bromine-containing DBPs induce higher cytotoxicity than chlorine-containing DBPs.

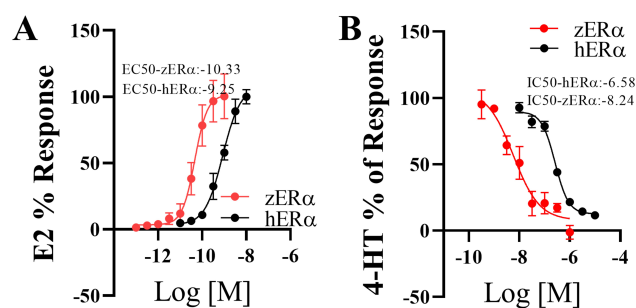


Fig. 2. *In vitro* assays of the estrogenic/anti-estrogenic activities of 17β -estradiol (E2) and 4-hydroxytamoxifen (HT). Estrogenic activity of E2 on both $ER\alpha$ s (A). The induction level at the maximum concentration of E2 (10 nM for h $ER\alpha$ and 1 nM for z $ER\alpha$) was set to 100%. Anti-estrogenic activity of HT on both $ER\alpha$ s (B). For this test, a fixed E2 concentration (1 nM E2 for h $ER\alpha$ and 0.1 nM E2 for z $ER\alpha$) was applied along with HT. The induction level of E2 was set to 100%. Data are presented as mean \pm standard deviation ($n = 3$).

3.2 Responses of $ER\alpha$ s to 17β -Estradiol and 4-Hydroxytamoxifen

We assessed estrogenic and anti-estrogenic activities between the two $ER\alpha$ s using selective ER modulators, namely E2 and HT, prior to testing for the endocrine disruption of DBPs. Dose-response curves illustrating the effects of E2 and HT on z $ER\alpha$ and h $ER\alpha$ are shown in Fig. 2. The EC_{50} values for E2 on z $ER\alpha$ and h $ER\alpha$ were 0.05 nM and 0.56 nM (Fig. 2A), respectively, while the half maximal inhibitory concentration (IC_{50}) values for HT were 0.006 μ M and 0.26 μ M (Fig. 2B). Although the EC_{50} and IC_{50} values showed 10–40 fold differences in responses between z $ER\alpha$ and h $ER\alpha$ due to the difference between hosts, their patterns and levels were similar to those of standard chemi-

Table 1. Comparison of half-maximal effective concentrations among organisms.

Chemical	Target organism	EC ₅₀ (M)	Reference
Iodoacetic acid (IAA)	Human embryonic kidney cell	5.3×10^{-6}	This study
	Salmonella Typhimurium	1.8×10^{-4}	[41]
	Salmonella Typhimurium	3.0×10^{-4}	[42]
	Saccharomyces cerevisiae	5.5×10^{-3}	[23]
	Human colorectal adenocarcinoma cell	3.4×10^{-5}	[43]
	Human colon epithelial cell	5.6×10^{-6}	[44]
	Human urothelial cell	2.4×10^{-5}	[45]
	Mouse neuroblastoma cell	2.7×10^{-5}	[46]
	Common carp hepatic microsomes	2.0×10^{-6}	[47]
	Retinal ganglion cells	6.0×10^{-6}	[48]
Rat cerebellar granule cell	9.8×10^{-6}	[49]	
Iodoacetamide (IAM)	Human embryonic kidney cell	4.3×10^{-6}	This study
	Saccharomyces cerevisiae	4.6×10^{-5}	[23]
	Pig kidney cell	5.0×10^{-6}	[50]
	Rat hepatocyte cell	6.0×10^{-6}	[50]
	Human hepatocyte cell	2.1×10^{-5}	[50]
	Human lymphocyte cell	5.0×10^{-6}	[50]
	Chinese hamster ovary cell	1.4×10^{-5}	[42]
	Human colon epithelial cell	3.9×10^{-5}	[44]
	Human gastric epithelial cell	4.3×10^{-6}	[51]
Human epidermal keratinocyte cell	3.9×10^{-5}	[51]	
Iodoacetonitrile (IAN)	Human embryonic kidney cell	5.3×10^{-6}	This study
	Saccharomyces cerevisiae	2.0×10^{-5}	[22]
	Chinese hamster ovary cell	3.3×10^{-6}	[52]
Chloroacetic acid (CAA)	Human embryonic kidney cell	1.0×10^{-4}	This study
	Salmonella Typhimurium	1.4×10^{-2}	[41]
	Salmonella Typhimurium	1.6×10^{-2}	[42]
	Saccharomyces cerevisiae	4.9×10^{-3}	[23]
	Human urothelial cell	7.9×10^{-4}	[45]
	Human colorectal adenocarcinoma cell	1.2×10^{-3}	[43]
	Chinese hamster ovary cell	8.1×10^{-4}	[20]
Chloroacetamide (CAM)	Human embryonic kidney cell	1.3×10^{-5}	This study
	Saccharomyces cerevisiae	4.9×10^{-3}	[23]
	Human gastric epithelial cell	1.0×10^{-4}	[51]
	Human epidermal keratinocyte cell	1.4×10^{-4}	[51]
	Chinese hamster ovary cell	1.5×10^{-4}	[42]
Chloroacetonitrile (CAN)	Human embryonic kidney cell	1.3×10^{-4}	This study
	Saccharomyces cerevisiae	5.3×10^{-3}	[23]
	Human liver cancer cell	5.5×10^{-2}	[20]
	Chinese hamster ovary cell	6.8×10^{-5}	[52]
Bromoacetic acid (BAA)	Human embryonic kidney cell	1.5×10^{-7}	This study
	Salmonella Typhimurium	9.6×10^{-4}	[41]
	Salmonella Typhimurium	8.8×10^{-4}	[42]
	Saccharomyces cerevisiae	6.4×10^{-3}	[23]
	Human urothelial cell	6.7×10^{-6}	[45]
	Human colorectal adenocarcinoma cell	4.2×10^{-5}	[43]
	Chinese hamster ovary cell	1.0×10^{-5}	[20]
Bromoacetamide (BAM)	Human embryonic kidney cell	5.1×10^{-6}	This study
	Saccharomyces cerevisiae	3.3×10^{-6}	[23]
	Human gastric epithelial cell	2.1×10^{-6}	[51]
	Human epidermal keratinocyte	3.3×10^{-6}	[51]
	Chinese hamster ovary cell	1.9×10^{-6}	[42]
Bromoacetonitrile (BAN)	Human embryonic kidney cell	5.7×10^{-6}	This study
	Saccharomyces cerevisiae	2.0×10^{-5}	[22]
	Human liver cancer cell	8.4×10^{-4}	[53]
	Chinese hamster ovary cell	3.2×10^{-6}	[52]

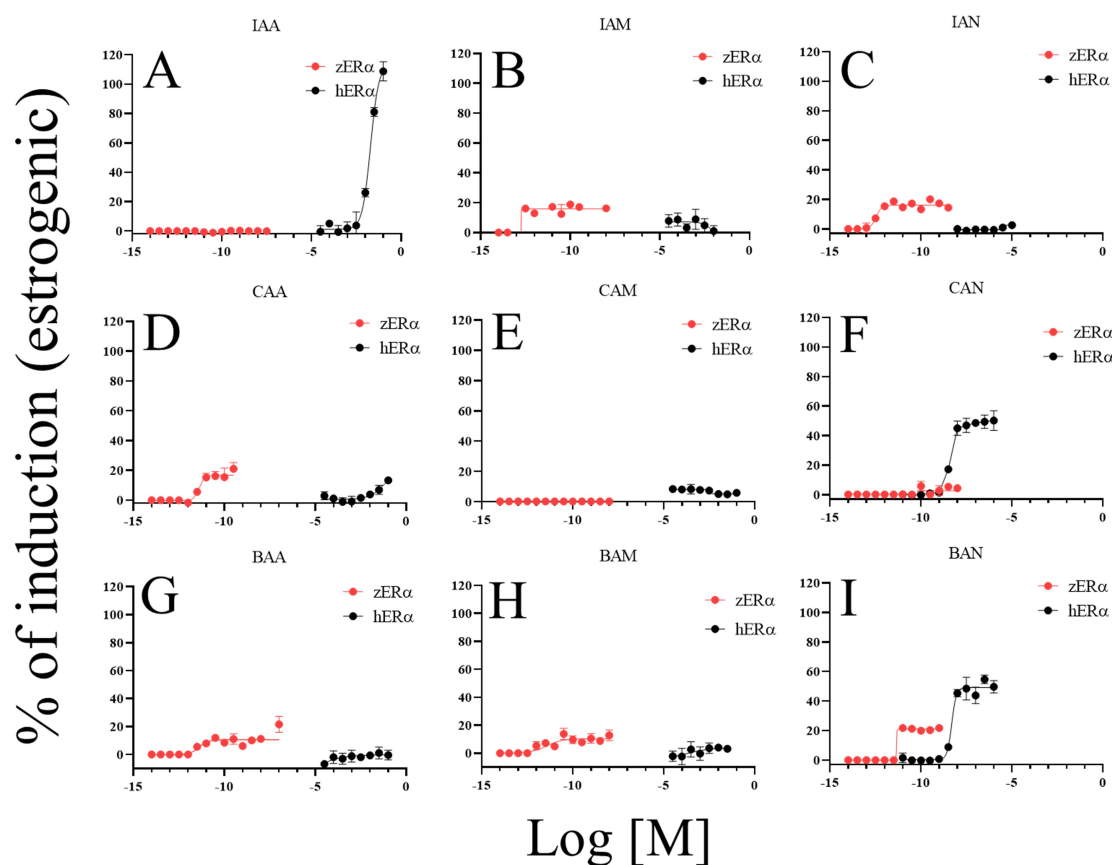


Fig. 3. Comparison of estrogenic activities among DBPs and between ER α s. Estrogenic activity of DBPs on both ER α s (A–I); IAA, iodoacetic acid (A); IAM, iodoacetamide (B); IAN, iodoacetonitrile (C); CAA, chloroacetic acid (D); CAM, chloroacetamide (E); CAN, chloroacetonitrile (F); BAA, bromoacetic acid (G); BAM, bromoacetamide (H); BAN, bromoacetonitrile (I). The induction level at the maximum concentration of 17 β -estradiol (E2; 10 nM for hER α and 1 nM for zER α) was set to 100% and induction levels of DBP were calculated as percentages relative to E2. Data are presented as mean \pm standard deviation (n = 4).

calcs. Furthermore, both ERs showed similar ligand interactions in terms of residues and binding energy in molecular docking analysis (Table 2). zER α -LBD had 20 interacting residues for E2, while hER α -LBD had 19 interacting residues. Especially, E2 formed the same hydrogen bond interactions with residues in each binding pocket site of both ERs. In light of these results, zER α and hER α showed a similar response upon E2 and HT exposure.

3.3 Dissimilar Ligand-Receptor Responses to DBPs between zER α and hER α

Although zER α and hER α have similar homology, they did not show identical responses to the DBPs in this study. In the estrogenic activity assessment shown in Fig. 3, IAA (108.7%), CAN (50.3%), and BAN (54.7%) showed significantly higher estrogenic effects on hER α than zER α . Meanwhile, other DBPs did not induce robust estrogenic activity in hER α . For zER α , some DBPs showed no or weak estrogenic activity (Fig. 3A,E,F). The maximum induction levels of other DBPs were 20.2% (CAA), 21.2% (BAA), 21.8% (BAN), 12.8% (BAM), 19.8% (IAN), and 18.9% (IAM). The anti-estrogenic activities were compared

(Fig. 4) and the patterns showed different responses, similar to the results of estrogenic activity assessment. IAM, CAM, and BAM showed anti-estrogenic activities on hER α . The ratios of the maximal inhibitory induction were 51.3% (IAM), 28.0% (CAM), and 29.5% (BAM). IAM exhibited the most potent activity. For zER α , IAA, CAM, and BAM showed anti-estrogenic activities. The ratios of maximum inhibitory induction were 59.8% (IAA), 51.9% (CAM), and 49.2% (BAM). CAM and BAM consistently exhibited anti-estrogenic activity in both ER α s.

CAA, CAM, BAM, and BAN showed identical response patterns for the two receptors. However, non-identical responses to some DBPs were observed. Notable dissimilarities were observed for IAA, IAM, and CAN. IAA had anti-estrogenic activity for zER α , but estrogenic activity for hER α (Figs. 3A,4A); IAM functioned as an estrogen for zER α , but as an intense anti-estrogen for hER α (Figs. 3B,4B); CAN caused no response in zER α but acted as an estrogen on hER α (Figs. 3F,4F). Therefore, we performed *in silico* molecular docking analysis to understand the differing estrogenic activities of DBPs between the two ER α s (Table 3 and **Supplementary Table**

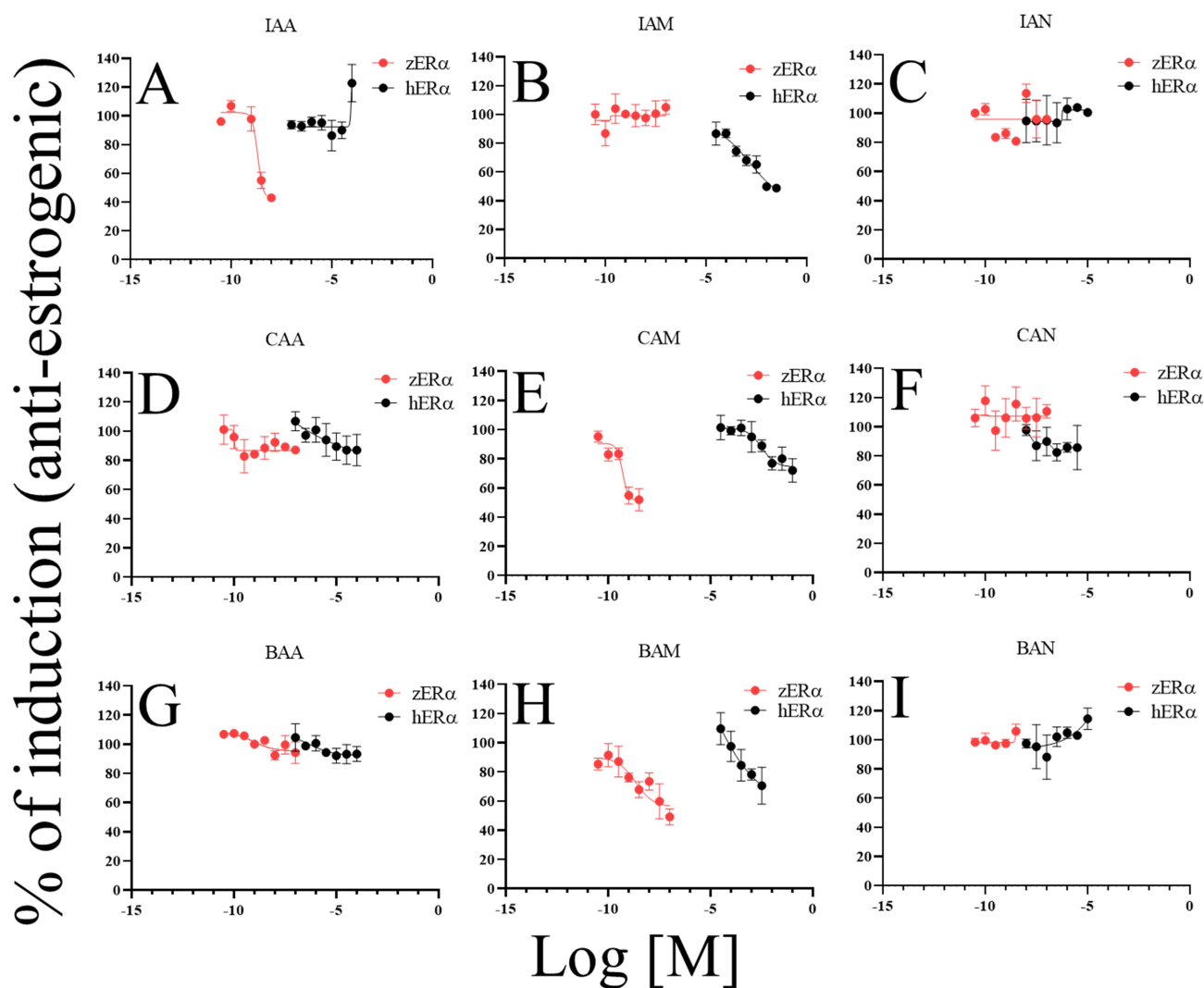


Fig. 4. Comparison of anti-estrogenic activities among DBPs and between ER α s. Anti-estrogenic activity of DBPs on both ER α s (A–I); IAA, iodoacetic acid (A); IAM, iodoacetamide (B); IAN, iodoacetoneitrile (C); CAA, chloroacetic acid (D); CAM, chloroacetamide (E); CAN, chloroacetoneitrile (F), BAA, bromoacetic acid (G); BAM, bromoacetamide (H); BAN, bromoacetoneitrile (I). For this test, the culture medium was supplemented with fixed concentrations of 17 β -estradiol (E2; 1 nM E2 for hER α and 0.1 nM E2 for zER α). The E2 induction levels were set to 100%. Data are presented as mean \pm standard deviation ($n = 4$).

1). The DBPs were successfully docked with zER α -LBD and hER α -LBD, respectively. All DBPs bonded to each model with similar binding free energies (-2.70 to -3.50 Kcal/mol). However, differences in the types and numbers of interactions, and orientations, were observed between the two models.

3.4 Correlation and Distance-Based Analyses of the Dissimilar Responses of two ER α s

In the comparison of estrogenic responses for each DBP, the activities of acetamide and acetonitrile compounds showed negative correlations between zER α and hER α (Fig. 5A). The DBPs with the largest negative correlation coefficients between zER α and hER α in the acetamide and acetonitrile classes were CAM (-0.68 ; p -value = 0.099, the null hypothesis is not statistically significant)

and CAN (-0.45 ; p -value = 0.664, the null hypothesis is not statistically significant), respectively (**Supplementary Table 2**). For acetic acid-based DBPs, both negative and positive correlations were found between the two ER α s. Responses to IAA were negatively correlated between zER α and hER α (-0.49 ; p -value = 0.168, the null hypothesis is not statistically significant), while CAA and BAA showed positive correlations between the two ER α s (**Supplementary Table 3**). Pearson's correlation coefficients for the anti-estrogenic responses indicated inconsistent and mixed correlations between the two ER α s for various DBPs (Fig. 5B).

The PCoA data showed general inter-species differences in terms of the responses of zER α and hER α (Fig. 5C). The two species were clearly separated on plots of the estrogenic responses. IAA, CAM, and CAN, which had no estrogenic effect on zER α , were plotted closer to the

Table 2. Binding free energies for docking between 17 β -estradiol (E2) and the ligand-binding domains of human and zebrafish estrogen receptor alpha.

Receptor	Ligand	Interacting residue number	Binding free energy (Kcal/mol)	Hydrogen bond interaction		Hydrophobic interaction		Van der Waals interaction	
				No.	Amino acids	No.	Amino acids	No.	Amino acids
zER α -LBD	E2	20	-10.7	3	Glu321, Arg362, His492	9	Leu314, Ala318, Leu352, Leu355, Met356, Leu359, Phe372, Ile392, Leu493	8	Met311, Thr315, Met317, Met389, Phe393, Leu396, Gly489, Met496
hER α -LBD	E2	19	-11.1	3	Glu353, Arg394, His524	9	Leu346, Ala350, Leu384, Leu387, Met388, Leu391, Phe404, Ile424, Leu525	7	Leu349, Leu384 Ile424, Phe425, Leu428, Gly521, Leu525

Table 3. Docking results between DBPs and ligand-binding domains of human and zebrafish estrogen receptor alpha.

Receptor	Interaction	Ligand								
		IAA	IAM	IAN	CAA	CAM	CAN	BAA	BAM	BAN
zER α -LBD	Interacting residues	7	10	8	7	9	9	8	9	8
	Binding free energy (Kcal/mol)	-3.50 \pm 0.00	-3.38 \pm 0.04	-2.90 \pm 0.00	-3.36 \pm 0.05	-3.30 \pm 0.00	-2.90 \pm 0.00	-3.40 \pm 0.00	-3.40 \pm 0.00	-2.90 \pm 0.00
	Hydrogen bond interaction	1	2	-	2	2	-	2	2	1
	Hydrophobic interaction	-	-	2	-	1	2	-	-	-
	Van der Waals interaction	6	8	6	5	6	7	6	7	7
hER α -LBD	Interacting residues	9	7	7	7	9	6	8	11	6
	Binding free energy (Kcal/mol)	-3.48 \pm 0.44	-3.32 \pm 0.04	-2.80 \pm 0.00	-3.48 \pm 0.10	-3.40 \pm 0.00	-2.70 \pm 0.00	-3.50 \pm 0.00	-3.34 \pm 0.05	-2.72 \pm 0.08
	Hydrogen bond interaction	2	1	1	2	2	1	1	1	1
	Hydrophobic interaction	-	-	3	-	-	3	-	-	3
	Van der Waals interaction	7	6	3	5	7	2	7	10	2

Table 4. Risk assessment results based on the effective concentrations.

Response	DBP	EC ₁₀ /IC ₁₀ (M)		EC ₅₀ /IC ₅₀ (M)		Risk assessment for endocrine disruption	
		zER	hER	zER	hER	Zebrafish	Human
Estrogenic activity	IAA	-	2.4 × 10 ⁻³	-	1.7 × 10 ⁻²	-	++
	IAM	2.3 × 10 ⁻¹³	-	-	-	+	-
	IAN	4.9 × 10 ⁻¹³	-	-	-	+	-
	CAA	5.5 × 10 ⁻¹²	5.2 × 10 ⁻²	-	-	+	+
	CAM	-	-	-	-	-	-
	CAN	-	1.1 × 10 ⁻⁹	-	3.2 × 10 ⁻⁷	-	++
	BAA	2.4 × 10 ⁻¹¹	-	-	-	+	-
	BAM	1.7 × 10 ⁻¹¹	-	-	-	+	-
	BAN	2.4 × 10 ⁻¹¹	2.1 × 10 ⁻⁹	-	1.0 × 10 ⁻⁷	+	++
Anti-estrogenic activity	IAA	1.2 × 10 ⁻⁹	-	6.0 × 10 ⁻⁹	-	++	-
	IAM	-	2.4 × 10 ⁻⁵	-	1.5 × 10 ⁻²	-	++
	IAN	-	-	-	-	-	-
	CAA	-	-	-	-	-	-
	CAM	6.2 × 10 ⁻¹¹	1.9 × 10 ⁻³	6.0 × 10 ⁻⁹	-	++	+
	CAN	-	-	-	-	-	-
	BAA	-	-	-	-	-	-
	BAM	1.4 × 10 ⁻¹⁰	2.5 × 10 ⁻⁴	1.5 × 10 ⁻⁷	-	++	+
	BAN	-	-	-	-	-	-

The symbol “++” indicates a strong response of DBPs calculated with both EC₁₀/IC₁₀ and EC₅₀/IC₅₀ values. The symbol “+” indicates a weak response of DBPs calculated with only EC₁₀/IC₁₀ values. The symbol “-” indicates the non-response of DBPs.

hER α than zER α group. As hER α had no or weak estrogenic responses to most DBPs, the PCoA plots for zER α interacting with IAA, CAM, and CAN were relatively similar to those for hER α (Figs. 3,5C). Meanwhile, the plots for zER α interacting with other DBPs clustered as a single group that showed clear separation from the points representing hER α . The anti-estrogenic results differed somewhat from the estrogenic PCoA results. The PCoA points were more dispersed than points on the estrogenic PCoA plots (Fig. 5C). The results were less regular than those for estrogenic PCoA plots, and the irregular pattern of anti-estrogenic responses corresponded well with the correlation coefficients (Fig. 5B,C).

3.5 Assessment of DBP Risks for Aquatic Animals

The EC₅₀ and IC₅₀ values represent the chemical concentrations that induce and inhibit a response halfway between the baseline and maximum response to exposure, respectively. According to those values, IAA, CAN and BAN caused robust estrogenic endocrine disruption in hER α , whereas all DBPs showed low levels of estrogenic endocrine disruption in zER α . IAA, CAM, and BAM showed robust anti-estrogenic endocrine disruption in zER α , whereas hER α was strongly affected by IAM (Table 4).

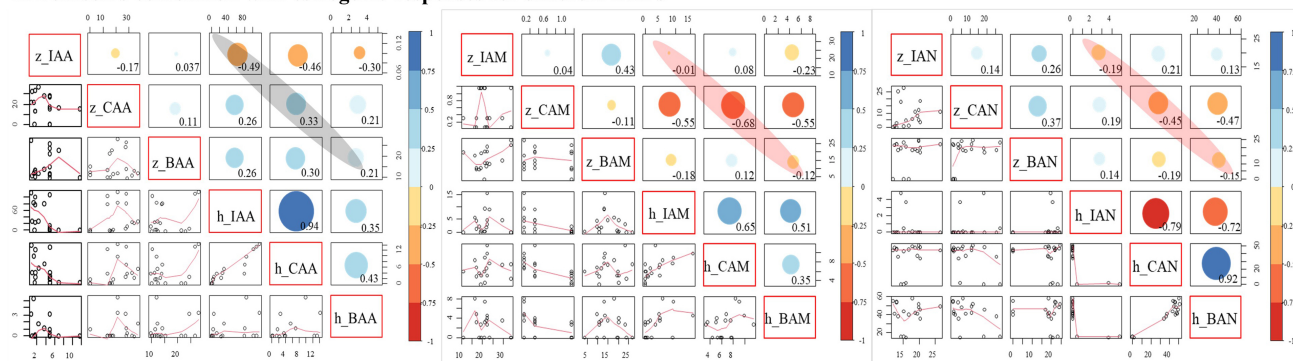
4. Discussion

In this study, we examined the effects of nine DBPs on zebrafish and human ER α s using *in vitro* reporter gene assay. Additionally, statistical analysis and molecular docking studies were employed to compare and understand ER α responses. The result of cell viability showed that DBPs

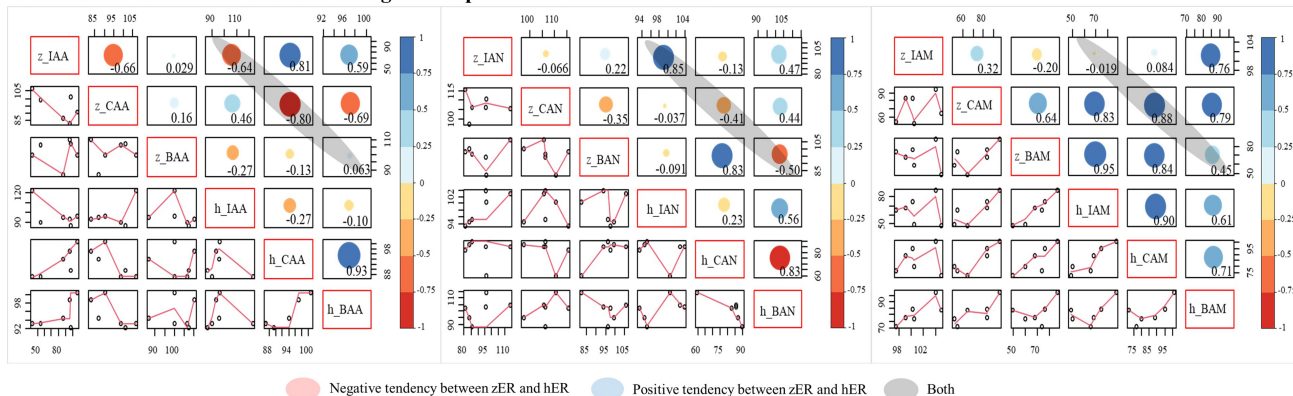
containing iodine and bromine have higher cytotoxicity than chlorine-containing DBPs. The cytotoxic effects of DBPs were similar to those described in previous studies that used other mammalian cell types [52,54]. The same trend was observed in *Salmonella typhimurium* and *Saccharomyces cerevisiae* [22,23,41,55]. Furthermore, toxicity has been tested in aquatic organisms, including algae, *Daphnia*, and zebrafish embryos [56–58]. The toxic effects of HAAs differed among organisms, as observed in the comparison of *Trimastix marina* (IAA > BAA > CAA), *Scenedesmus* sp. (CAA > BAA > IAA), *Daphnia magna* (IAA > BAA > CAA), and zebrafish embryos (CAA > BAA > IAA). HANs showed the same toxicity trend as HAAs in those organisms, while HAMS caused the same pattern of toxicity as HAAs in zebrafish embryos. These facts indicate that DBPs can seriously affect aquatic biota, and bromine- and iodine-containing DBPs induce greater toxicity than chlorine-containing DBPs.

The results of the reporter gene assay showed that DBPs induced estrogenic and anti-estrogenic effects on the two ER α s. Interestingly, notable dissimilarities between the two ER α s were observed for some DBPs. Thus, we applied molecular docking analysis to understand the differing estrogenic activities of DBPs between the two ER α s. Molecular docking analysis offers binding free energy, interaction types, and the orientations of the ligand and target receptor. Hence, molecular docking underlies fundamental molecular mechanisms and has been actively used in comprehensive studies to evaluate potential endocrine disruption [59,60]. Our previous study reported the same pattern of estrogenic activity in those two ER α s upon exposure to E2. Furthermore, high sequence similarity (78%) was

A-Pearson's correlation with estrogenic responses for different DBPs



B-Pearson's correlation with anti-estrogenic responses for different DBPs



C-PCoA for estrogenic and anti-estrogenic responses

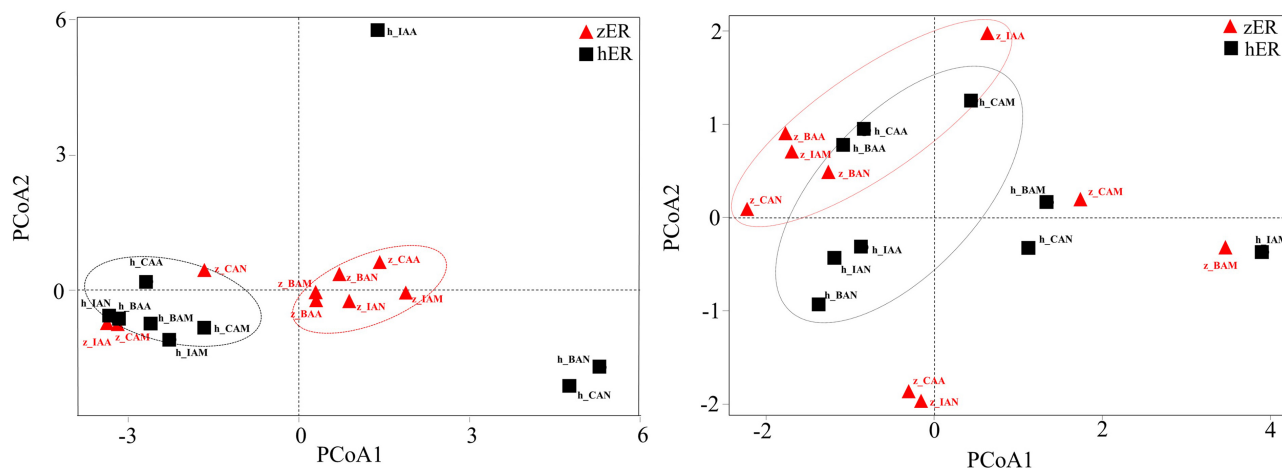


Fig. 5. Correlation and Principal Coordinate Analyses. Results of statistical analysis of the estrogenic responses (A) and the anti-estrogenic responses (B) to various DBPs. Principal coordinate analysis (PCoA) of zER α and hER α : estrogenic responses and anti-estrogenic responses to various DBPs (C).

identified between the two LBD regions, and E2 interacted through hydrogen bonds with certain residues (Glu353, Arg394, and His524 of hER α -LBD and Glu321, Arg362, and His492 of zER α -LBD) [34]; these interactions correspond to the results of the present study as well as a previously reported docking analysis [61]. In particular, His524 is one of the primary residues in the hER 515–535 region, and the primary residues are responsible for ligand binding and recognition. In addition, hydrogen bonds drive the

selective interactions that underpin molecular recognition of the receptors and determine protein folding and structure [62]. As shown in Table 3 and **Supplementary Table 1**, the DBPs were successfully docked with zER α -LBD and hER α -LBD, respectively. The results revealed common features that support the interpretation of the *in vitro* results. IAA, CAN, and BAN, which showed estrogenic activities with hER α , interacted with the His524 residue via a hydrogen bond. For zER α , BAN, IAN, CAM, and BAM

exhibited weak estrogenic activities, while BAN and IAN interacted with His492 via a hydrogen bond and Van der Waals interaction, respectively. Although CAA and BAA did not interact with this residue via hydrogen bonding, hydrogen bond interactions with other residues, such as the E2/zER α -LBD complex, formed. As noted in the previous section, primary residues such as His524 are responsible for binding and recognition of the ligand [63], as confirmed by our previous study of the same two ER α s using BPA and its analogs [34]. Thus, interactions between DBPs and the primary residues appear to induce ligand binding and recognition, eventually resulting in estrogenic activity.

In the case of anti-estrogenic activity, it is difficult to define the activity based on interactions with specific residues and binding free energy due to the diverse modes of action driving anti-estrogenic effects [64]. However, two features were observed in the docking complexes that showed DBP-induced anti-estrogenic activity in this study. First, the DBPs interacted in different orientations with residues in the binding pocket compared to the estrogens. CAM and BAM formed hydrogen bonds with Val354 and Lys417 in the zER α -LBD. In the hER α -LBD, CAM interacted with Glu353 and Leu387 via hydrogen bonds, while BAM interacted with Thr347 via a hydrogen bond. Second, DBPs that interact only with glycine residues (Gly321 for zER α -LBD and Gly353 for hER α -LBD) via hydrogen bonds exhibited anti-estrogenic activity. These features have been observed for other chemicals in previous studies [65,66]. Chen *et al.* [66] reported that bisphenol AF and perfluorooctanoic acid could compete for common key residues, such as Glu321 and Arg362, in the binding pocket of zER α , and induce anti-estrogenic effects. Cao *et al.* [65] reported the binding of bisphenol analogs to residue Thr347 of hER α via a hydrogen bond, suggesting that the binding mode may be a major factor underlying reduced estrogenic activities through allosteric effects. Based on these results, we speculate that anti-estrogenic DBPs have different or inappropriate orientations when interacting with residues in the binding pocket, resulting in anti-estrogen effects on both receptors. Meanwhile, BAM exhibited weak estrogenic and anti-estrogenic activities when applied to zER α . Such double-directional endocrine-disrupting effects on an ER have been observed previously for some chemicals. Phloridzin and protocatechuic acid have double-directional endocrine-disrupting effects on proliferation of the MCF-7 cell line [67,68]. When the intracellular environment lacks endogenous estrogen, these double-directional EDCs show estrogen-like effects in cells, whereas the same EDCs can exhibit anti-estrogenic activities in the presence of sufficient estrogen. These chemicals have been proposed for use as alternatives to estrogen therapy to overcome the associated side effects, however, the double-directional effect of EDCs still can adversely influence the endocrine systems of organisms.

This study employed Pearson's correlation coefficient

and PCoA to compare responses between zER α and hER α [69,70]. Pearson's correlation coefficient has limited use for visualizing the myriad interactions of multiple DBPs with two ER α s, as it can only assess such relationships for individual DBPs. The statistical significances of each Pearson's correlation co-existed. This means that both statistically significant and non-significant points are shown. Therefore, further statistical analysis was required to explore the general trends. The two species were clearly separated on plots of the estrogenic responses. The anti-estrogenic results differed somewhat from the estrogenic PCoA results. The results were less regular than those for estrogenic PCoA plots. These facts indicate that the same DBP can induce completely different patterns of endocrine disruption among species of biota, indicating that risk assessment for DBPs should be conducted for each environment and organism exposed to DBPs. Among DBPs, IAA showed the most distinctive effects between zER α and hER α . This was the largest disparity in this study. IAA, which showed the most potent endocrine disruption, has cytotoxic and genotoxic effects on mammalian cells [20,43,71], and served as an endocrine disruptor of the thyroid endocrine system in a study using a rat pituitary-derived cell line [72]. On the other hand, CAN and BAN, which had estrogenic activity when applied to hER α , have mutagenic, carcinogenic, and histopathological effects in mice [73–75]. Our previous study demonstrated the effect of estrogenic endocrine disruption on hER α [22,23], while these substances had no or weak estrogenic effects on zER α . In terms of anti-estrogenic endocrine-disrupting effects, CAM and BAM acted as strongly anti-estrogenic compounds on zER α in this study. CAM, which is widely used worldwide as a pesticide and thus is frequently present in surface water, causes strong thyroid hormone disruption in aquatic organisms [76]. Furthermore, BAM can disrupt thyroid hormone homeostasis and cause developmental toxicity in zebrafish [77]. IAA, which had the strongest effects among DBPs in this study, causes pericardial edema, fin malformations, and delayed development in zebrafish [78]. This study found that although CAM and BAM did not cause robust endocrine disruption in hER α , they caused anti-estrogenic endocrine disruption in zER α . Anti-estrogenic endocrine disruption can lead to adverse outcomes, including alteration of the sex ratio and inhibition of normal ER-mediated ovarian development in fish [79,80]. DBP emitted from WWTPs into freshwater environments is more likely to have adverse effects on aquatic organisms than on humans, as WWTPs discharge their final effluent directly into rivers. Taken together, our results indicate that DBPs can disrupt the endocrine systems of both zebrafish and humans. These findings suggest that DBPs could possibly affect the endocrine system of aquatic biota. However, further research is necessary to confirm these functions *in vivo* and investigate the reproductive toxicity of DBPs on endocrine systems.

5. Conclusions

To the best of our knowledge, this is the first study to compare endocrine responses to halogenated DBPs between zER α and hER α . We explored the cytotoxicity and endocrine disruption of nine DBPs, focusing on halogenated DBPs, and revealed the differing responses using correlation and distance-based analyses based on reporter assay data for two ER α s. Among the nine types of DBPs, IAA, CAN, and BAN triggered estrogenic activities in hER α . Meanwhile, IAA, CAM, and BAM inhibited estrogenic activities of E2 in zER α . The effective concentrations of DBP used in this study are frequently detected in effluent from WWTPs and aquatic environments. Aquatic organisms, specifically fish, are exposed to effective concentrations of DBPs throughout their life, and are thus more affected by endocrine disruption than humans. Therefore, this study suggests that endocrine-disrupting effects of toxic substances should be evaluated separately in multiple species.

Availability of Data and Materials

The datasets used and/or analyzed during the current study are available from the corresponding author on reasonable request.

Author Contributions

SAL and CGP wrote original drafting of the manuscript, SAL, CGP, JHY and YJK designed the research and conceptualization. SAL and CGP performed the research. SAL, CGP, IC, CSR analyzed the data. YJK and ME performed review & editing. JHY acquired funding & administrated the project. All authors read and approved the final manuscript.

Ethics Approval and Consent to Participate

Not applicable.

Acknowledgment

The authors would like to acknowledge Dr. Da-Hye Kim at the University of Antwerp for conducting the precedent research.

Funding

This study endowed research award from Next&Bio Inc., by the Strategies for Establishing Adverse outcome pathways (AOPs) use in alternatives to animal testing and their global standardization (No. 32201).

Conflict of Interest

The authors declare no conflict of interest. Next&Bio Inc. declare no competing financial interests and this paper is written for non-commercial purposes.

Supplementary Material

Supplementary material associated with this article can be found, in the online version, at <https://doi.org/10.31083/j.fbl2803048>.

References

- [1] Bogler A, Packman A, Furman A, Gross A, Kushmaro A, Ronen A, *et al.* Rethinking wastewater risks and monitoring in light of the COVID-19 pandemic. *Nature Sustainability*. 2020; 3: 981–990.
- [2] Mezzanotte V, Antonelli M, Citterio S, Nurizzo C. Wastewater disinfection alternatives: chlorine, ozone, peracetic acid, and UV light. *Water Environment Research*. 2007; 79: 2373–2379.
- [3] Hua Z, Li D, Wu Z, Wang D, Cui Y, Huang X, *et al.* DBP formation and toxicity alteration during UV/chlorine treatment of wastewater and the effects of ammonia and bromide. *Water Research*. 2021; 188: 116549.
- [4] Ding H, Meng L, Zhang H, Yu J, An W, Hu J, *et al.* Occurrence, profiling and prioritization of halogenated disinfection by-products in drinking water of China. *Environmental Science. Processes & Impacts*. 2013; 15: 1424–1429.
- [5] Carter RAA, Allard S, Croué JP, Joll CA. Occurrence of disinfection by-products in swimming pools and the estimated resulting cytotoxicity. *The Science of the Total Environment*. 2019; 664: 851–864.
- [6] Ratpukdi T, Sinorak S, Kiattisaksiri P, Punyapalakul P, Siripattanakul-Ratpukdi S. Occurrence of trihalomethanes and haloacetonitriles in water distribution networks of Khon Kaen Municipality, Thailand. *Water Supply*. 2019; 19: 1748–1757.
- [7] Lau SS, Wei X, Bokenkamp K, Wagner ED, Plewa MJ, Mitch WA. Assessing Additivity of Cytotoxicity Associated with Disinfection Byproducts in Potable Reuse and Conventional Drinking Waters. *Environmental Science & Technology*. 2020; 54: 5729–5736.
- [8] Anglada A, Urriaga A, Ortiz I, Mantzavinos D, Diamadopoulos E. Boron-doped diamond anodic treatment of landfill leachate: evaluation of operating variables and formation of oxidation by-products. *Water Research*. 2011; 45: 828–838.
- [9] Jones, SA. Environmental Protection Agency: national primary drinking water regulations: stage 2 disinfectants and disinfection byproducts rule. *Community Dental Health*. 2006; 29: 195–197.
- [10] Issa HM. Comparative Analysis of Different Disinfection Techniques Performances in Drinking Water Treatment Plant Using a Process Simulation Software. *Zanco Journal of Pure and Applied Sciences*. 2019; 31: 1–8.
- [11] Eiseheid AC, Meyer JN, Linden KG. UV disinfection of adenoviruses: molecular indications of DNA damage efficiency. *Applied and Environmental Microbiology*. 2009; 75: 23–28.
- [12] Kong J, Lu Y, Ren Y, Chen Z, Chen M. The virus removal in UV irradiation, ozonation and chlorination. *Water Cycle*. 2021; 2: 23–31.
- [13] Edwards-Brandt J, Shorney-Darby H, Neemann J, Hesby J, Tona C. Use of Ozone for Disinfection and Taste and Odor Control at Proposed Membrane Facility. *Ozone: Science & Engineering*. 2007; 29: 281–286.
- [14] Richardson SD. Disinfection by-products and other emerging contaminants in drinking water. *TrAC Trends in Analytical Chemistry*. 2003; 22: 666–684.
- [15] Weinberg H, Krasner S, Richardson S, Thruston A. The Occurrence of Disinfection By-Products (DBPs) of Health Concern in Drinking Water: Results of a Nationwide DBP Occurrence Study. U.S. Environmental Protection Agency National Exposure Research Laboratory: Athens GA. 2002.
- [16] Hua G, Yeats S. Control of trihalomethanes in wastewater treat-

- ment. Florida Water Resources Journal. 2010; 4: 6–12.
- [17] Vu TN, Kimura SY, Plewa MJ, Richardson SD, Mariñas BJ. Predominant N-Haloacetamide and Haloacetonitrile Formation in Drinking Water via the Aldehyde Reaction Pathway. *Environmental Science & Technology*. 2019; 53: 850–859.
- [18] Zhao H, Yang L, Li Y, Xue W, Li K, Xie Y, *et al.* Environmental occurrence and risk assessment of haloacetic acids in swimming pool water and drinking water. *RSC Advances*. 2020; 10: 28267–28276.
- [19] Wei X, Yang M, Zhu Q, Wagner ED, Plewa MJ. Comparative Quantitative Toxicology and QSAR Modeling of the Haloacetonitriles: Forcing Agents of Water Disinfection Byproduct Toxicity. *Environmental Science & Technology*. 2020; 54: 8909–8918.
- [20] Plewa MJ, Simmons JE, Richardson SD, Wagner ED. Mammalian cell cytotoxicity and genotoxicity of the haloacetic acids, a major class of drinking water disinfection by-products. *Environmental and Molecular Mutagenesis*. 2010; 51: 871–878.
- [21] Dong F, Chen J, Li C, Ma X, Jiang J, Lin Q, *et al.* Evidence-based analysis on the toxicity of disinfection byproducts *in vivo* and *in vitro* for disinfection selection. *Water Research*. 2019; 165: 114976.
- [22] Park CG, Jung KC, Kim DH, Kim YJ. Monohaloacetonitriles induce cytotoxicity and exhibit different mode of action in endocrine disruption. *The Science of the Total Environment*. 2021; 761: 143316.
- [23] Kim DH, Park CG, Kim YJ. Characterizing the potential estrogenic and androgenic activities of two disinfection byproducts, mono-haloacetic acids and haloacetamides, using *in vitro* bioassays. *Chemosphere*. 2020; 242: 125198.
- [24] Barkhem T, Nilsson S, Gustafsson JA. Molecular mechanisms, physiological consequences and pharmacological implications of estrogen receptor action. *American Journal of Pharmacogenomics: Genomics-related Research in Drug Development and Clinical Practice*. 2004; 4: 19–28.
- [25] Hewitt SC, Winuthayanon W, Korach KS. What’s new in estrogen receptor action in the female reproductive tract. *Journal of Molecular Endocrinology*. 2016; 56: R55–71.
- [26] Kovats S. Estrogen receptors regulate innate immune cells and signaling pathways. *Cellular Immunology*. 2015; 294: 63–69.
- [27] Shen M, Shi H. Sex Hormones and Their Receptors Regulate Liver Energy Homeostasis. *International Journal of Endocrinology*. 2015; 2015: 294278.
- [28] Diamanti-Kandarakis E, Bourguignon JP, Giudice LC, Hauser R, Prins GS, Soto AM, *et al.* Endocrine-disrupting chemicals: an Endocrine Society scientific statement. *Endocrine Reviews*. 2009; 30: 293–342.
- [29] La Merrill MA, Vandenberg LN, Smith MT, Goodson W, Browne P, Patisaul HB, *et al.* Consensus on the key characteristics of endocrine-disrupting chemicals as a basis for hazard identification. *Nature Reviews. Endocrinology*. 2020; 16: 45–57.
- [30] Faheem M, Bhandari RK. Detrimental Effects of Bisphenol Compounds on Physiology and Reproduction in Fish: A Literature Review. *Environmental Toxicology and Pharmacology*. 2021; 81: 103497.
- [31] Kar S, Sangem P, Anusha N, Senthilkumaran B. Endocrine disruptors in teleosts: Evaluating environmental risks and biomarkers. *Aquaculture and Fisheries*. 2021; 6: 1–26.
- [32] Schartl M. Beyond the zebrafish: diverse fish species for modeling human disease. *Disease Models & Mechanisms*. 2014; 7: 181–192.
- [33] Phillips C, Roberts LR, Schade M, Bazin R, Bent A, Davies NL, *et al.* Design and structure of stapled peptides binding to estrogen receptors. *Journal of the American Chemical Society*. 2011; 133: 9696–9699.
- [34] Park CG, Singh N, Ryu CS, Yoon JY, Esterhuizen M, Kim YJ. Species Differences in Response to Binding Interactions of Bisphenol A and its Analogs with the Modeled Estrogen Receptor 1 and *In Vitro* Reporter Gene Assay in Human and Zebrafish. *Environmental Toxicology and Chemistry*. 2022; 41: 2431–2443.
- [35] Webb B, Sali A. Protein Structure Modeling with MODELLER. *Methods in Molecular Biology (Clifton, N.J.)*. 2017; 1654: 39–54.
- [36] Shen MY, Sali A. Statistical potential for assessment and prediction of protein structures. *Protein Science: a Publication of the Protein Society*. 2006; 15: 2507–2524.
- [37] Colovos C, Yeates TO. Verification of protein structures: patterns of nonbonded atomic interactions. *Protein Science: a Publication of the Protein Society*. 1993; 2: 1511–1519.
- [38] Laskowski RA, MacArthur MW, Thornton JM. PROCHECK: validation of protein-structure coordinates. In *International Tables for Crystallography* (pp. 684–687). International Union of Crystallography: Chester, UK. 2012.
- [39] Wiederstein M, Sippl MJ. ProSA-web: interactive web service for the recognition of errors in three-dimensional structures of proteins. *Nucleic Acids Research*. 2007; 35: W407–W410.
- [40] Trott O, Olson AJ. AutoDock Vina: improving the speed and accuracy of docking with a new scoring function, efficient optimization, and multithreading. *Journal of Computational Chemistry*. 2010; 31: 455–461.
- [41] Zhang SH, Miao DY, Tan L, Liu AL, Lu WQ. Comparative cytotoxic and genotoxic potential of 13 drinking water disinfection by-products using a microplate-based cytotoxicity assay and a developed SOS/umu assay. *Mutagenesis*. 2016; 31: 35–41.
- [42] Plewa MJ, Muellner MG, Richardson SD, Fasano F, Buettner KM, Woo YT, *et al.* Occurrence, synthesis, and mammalian cell cytotoxicity and genotoxicity of haloacetamides: an emerging class of nitrogenous drinking water disinfection byproducts. *Environmental science & technology*. 2008; 42: 955–961.
- [43] Procházka E, Escher BI, Plewa MJ, Leusch FD. In Vitro Cytotoxicity and Adaptive Stress Responses to Selected Haloacetic Acid and Halobenzoquinone Water Disinfection Byproducts. *Chemical research in toxicology*. 2015; 28: 2059–2068.
- [44] Sayess R, Khalil A, Shah M, Reckhow DA, Godri Pollitt KJ. Comparative Cytotoxicity of Six Iodinated Disinfection Byproducts on Nontransformed Epithelial Human Colon Cells. *Environmental Science & Technology Letters*. 2017; 4: 143–148.
- [45] Marsà A, Cortés C, Hernández A, Marcos R. Hazard assessment of three haloacetic acids, as byproducts of water disinfection, in human urothelial cells. *Toxicology and Applied Pharmacology*. 2018; 347: 70–78.
- [46] Andrés MI, Repetto G, Sanz P, Repetto M. Comparative effects of the metabolic inhibitors 2,4-dinitrophenol and iodoacetate on mouse neuroblastoma cells *in vitro*. *Toxicology*. 1996; 110: 123–132.
- [47] Noyes PD, Kelly SM, Mitchelmore CL, Stapleton HM. Characterizing the *in vitro* hepatic biotransformation of the flame retardant BDE 99 by common carp. *Aquatic Toxicology*. 2010; 97: 142–150.
- [48] Ondricek AJ, Kashyap AK, Thamma SI, Vishwanatha JK. A comparative study of phytoestrogen action in mitigating apoptosis induced by oxidative stress. *In Vivo*. 2012; 26: 765–775.
- [49] Malcolm CS, Benwell KR, Lamb H, Bebbington D, Porter RH. Characterization of iodoacetate-mediated neurotoxicity *in vitro* using primary cultures of rat cerebellar granule cells. *Free Radical Biology and Medicine*. 2000; 28: 102–107.
- [50] Bedard K, MacDonald N, Collins J, Cribb A. Cytoprotection following endoplasmic reticulum stress protein induction in continuous cell lines. *Basic & clinical pharmacology & toxicology*. 2004; 94: 124–131.
- [51] Ding X, Zhu J, Wang X, Zhou W, Wu K, Zhou Z, *et al.* Different

- cytotoxicity of disinfection by-product haloacetamides on two exposure pathway-related cell lines: Human gastric epithelial cell line GES-1 and immortalized human keratinocyte cell line HaCaT. *Science of The Total Environment*. 2019; 692: 1267–1275.
- [52] Muellner MG, Wagner ED, McCalla K, Richardson SD, Woo YT, Plewa MJ. Haloacetamides vs. regulated haloacetic acids: are nitrogen-containing DBPs more toxic? *Environmental science & technology*. 2007; 41: 645–651.
- [53] Lu G, Qin D, Wang Y, Liu J, Chen W. Single and combined effects of selected haloacetamides in a human-derived hepatoma line. *Ecotoxicology and Environmental Safety*. 2018; 163: 417–426.
- [54] Wagner ED, Plewa MJ. CHO cell cytotoxicity and genotoxicity analyses of disinfection by-products: an updated review. *Journal of Environmental Sciences*. 2017; 58: 64–76.
- [55] Plewa MJ, Wagner ED, Richardson SD, Thruston AD, Woo YT, McKague AB. Chemical and biological characterization of newly discovered iodoacid drinking water disinfection byproducts. *Environmental Science & Technology*. 2004; 38: 4713–4722.
- [56] Liu J, Zhang X. Comparative toxicity of new halophenolic DBPs in chlorinated saline wastewater effluents against a marine alga: halophenolic DBPs are generally more toxic than haloaliphatic ones. *Water Research*. 2014; 65: 64–72.
- [57] Hanigan D, Truong L, Simonich M, Tanguay R, Westerhoff P. Zebrafish embryo toxicity of 15 chlorinated, brominated, and iodinated disinfection by-products. *Journal of Environmental Sciences*. 2017; 58: 302–310.
- [58] Cui H, Chen B, Jiang Y, Tao Y, Zhu X, Cai Z. Toxicity of 17 disinfection by-products to different trophic levels of aquatic organisms: ecological risks and mechanisms. *Environmental Science & Technology*. 2021; 55: 10534–10541.
- [59] Babu S, Vellore NA, Kasibotla AV, Dwayne HJ, Stubblefield MA, Uppu RM. Molecular docking of bisphenol A and its nitrated and chlorinated metabolites onto human estrogen-related receptor-gamma. *Biochemical and Biophysical Research Communications*. 2012; 426: 215–220.
- [60] Guedes IA, de Magalhães CS, Dardenne LE. Receptor–ligand molecular docking. *Biophysical Reviews*. 2014; 6: 75–87.
- [61] Asnake S, Modig C, Olsson P-E. Species differences in ligand interaction and activation of estrogen receptors in fish and human. *The Journal of steroid biochemistry and molecular biology*. 2019; 195: 105450.
- [62] Hubbard RE, Haider MK. Hydrogen bonds in proteins: role and strength. In: eLS, J. M. Valpuesta (ed). John Wiley & Sons: Chichester, UK. 2010.
- [63] Ekena K, Weis KE, Katzenellenbogen JA, Katzenellenbogen BS. Identification of amino acids in the hormone binding domain of the human estrogen receptor important in estrogen binding. *Journal of Biological Chemistry*. 1996; 271: 20053–20059.
- [64] Dougall IG, Unitt J. Evaluation of the biological activity of compounds: techniques and mechanism of action studies. In *The Practice of Medicinal Chemistry* (pp. 15–43). Elsevier: London, UK. 2015.
- [65] Cao H, Wang F, Liang Y, Wang H, Zhang A, Song M. Experimental and computational insights on the recognition mechanism between the estrogen receptor α with bisphenol compounds. *Archives of toxicology*. 2017; 91: 3897–3912.
- [66] Chen P, Wang Q, Chen M, Yang J, Wang R, Zhong W, et al. Antagonistic Estrogenic Effects Displayed by Bisphenol AF and Perfluorooctanoic Acid on Zebrafish (*Danio rerio*) at an Early Developmental Stage. *Environmental Science & Technology Letters*. 2018; 5: 655–661.
- [67] Wang J, Chung MH, Xue B, Ma H, Ma C, Hattori M. Estrogenic and antiestrogenic activities of phloridzin. *Biological and Pharmaceutical Bulletin*. 2010; 33: 592–597.
- [68] Hu F, Wang J, Luo H, Zhang L, Luo Y, Sun W, et al. Estrogenic and antiestrogenic activities of protocatechic acid. In *Frontier and Future Development of Information Technology in Medicine and Education* (pp. 3319–3327). Springer: Dordrecht, Netherlands. 2014.
- [69] Pearson ES. The test of significance for the correlation coefficient. *Journal of the American Statistical Association*. 1931; 26: 128–134.
- [70] Jolliffe IT. Discarding variables in a principal component analysis. I: Artificial data. *Journal of the Royal Statistical Society: Series C (Applied Statistics)*. 1972; 21: 160–173.
- [71] Zhang SH, Miao DY, Liu AL, Zhang L, Wei W, Xie H, et al. Assessment of the cytotoxicity and genotoxicity of haloacetic acids using microplate-based cytotoxicity test and CHO/HGPRT gene mutation assay. *Mutation Research/Genetic Toxicology and Environmental Mutagenesis*. 2010; 703: 174–179.
- [72] Xia Y, Mo Y, Yang Q, Yu Y, Jiang M, Wei S, et al. Iodoacetic acid disrupting the thyroid endocrine system in vitro and in vivo. *Environmental Science & Technology*. 2018; 52: 7545–7552.
- [73] Muller-Pillet V, Joyeux M, Ambroise D, Hartemann P. Genotoxic activity of five haloacetamides: comparative investigations in the single cell gel electrophoresis (comet) assay and the Ames-fluctuation test. *Environmental and molecular mutagenesis*. 2000; 36: 52–58.
- [74] Attia S, Ahmad S, Zoheir K, Bakheet S, Helal G, Abd-Allah A, et al. Genotoxic evaluation of chloroacetamide in murine marrow cells and effects on DNA damage repair gene expressions. *Mutagenesis*. 2014; 29: 55–62.
- [75] Deng Y, Zhang Y, Lu Y, Lu K, Bai H, Ren H. Metabolomics evaluation of the in vivo toxicity of bromoacetamides: One class of high-risk nitrogenous disinfection byproducts. *Science of The Total Environment*. 2017; 579: 107–114.
- [76] Xu C, Sun X, Niu L, Yang W, Tu W, Lu L, et al. Enantioselective thyroid disruption in zebrafish embryo-larvae via exposure to environmental concentrations of the chloroacetamide herbicide acetochlor. *Science of The Total Environment*. 2019; 653: 1140–1148.
- [77] Wang W, Ma Q, Ding X, Xu Y, He M, Xu J, et al. Developmental toxicity of bromoacetamide via the thyroid hormone receptors-mediated disruption of thyroid hormone homeostasis in zebrafish embryos. *Ecotoxicology and Environmental Safety*. 2022; 233: 113334.
- [78] Teixidó E, Piqué E, Gonzalez-Linares J, Llobet JM, Gómez-Catalán J. Developmental effects and genotoxicity of 10 water disinfection by-products in zebrafish. *Journal of Water and Health*. 2015; 13: 54–66.
- [79] Kawahara T, Yamashita I. Estrogen-independent ovary formation in the medaka fish, *Oryzias latipes*. *Zoological science*. 2000; 17: 65–68.
- [80] Andersen L, Kinnberg K, Holbech H, Korsgaard B, Bjerregaard P. Evaluation of a 40 day assay for testing endocrine disruptors: effects of an anti-estrogen and an aromatase inhibitor on sex ratio and vitellogenin concentrations in juvenile zebrafish (*Danio rerio*). *Fish Physiology and Biochemistry*. 2004; 30: 257–266.